


RESEARCH ARTICLE

Tractography of sensorimotor pathways in dyskinetic cerebral palsy: Association with motor function

Xavier Caldu^{1,2,3} , Lee B. Reid⁴, Kerstin Pannek⁵, Jurgen Fripp⁵, Júlia Ballester-Plané^{1,2,3}, David Leiva^{2,6}, Roslyn N. Boyd⁷, Roser Pueyo^{1,2,3} & Olga Laporta-Hoyos^{1,2,3}

¹Departament de Psicologia Clínica i Psicobiologia, Universitat de Barcelona, Pg. Vall d'Hebron, 171, Barcelona, 08035, Spain

²Institut de Neurociències, Universitat de Barcelona, Barcelona, Spain

³Institut de Recerca Sant Joan de Déu, Esplugues de Llobregat, Spain

⁴Department of Psychiatry, University of California San Francisco, San Francisco, California, USA

⁵Australian E-Health Research Centre, CSIRO, Brisbane, Queensland, Australia

⁶Departament de Psicologia Social i Psicologia Quantitativa, Universitat de Barcelona, Barcelona, Spain

⁷Queensland Cerebral Palsy and Rehabilitation Research Centre, Faculty of Medicine, The University of Queensland, Brisbane, Queensland, Australia

Correspondence

Roser Pueyo, Departament de Psicologia Clínica i Psicobiologia, Universitat de Barcelona, Campus Mundet, Ponent. Passeig de la Vall d'Hebron, 171, Barcelona 08035, Spain. Tel: 933125053; Fax: 934021584; E-mail: rpueyo@ub.edu

Received: 13 March 2024; Revised: 13 June 2024; Accepted: 22 July 2024

Annals of Clinical and Translational Neurology 2024; 11(10): 2609–2622

doi: 10.1002/acn3.52174

Abstract

Objectives: Neuroimaging studies of dyskinetic cerebral palsy (CP) are scarce and the neuropathological underpinnings are not fully understood. We delineated the corticospinal tract (CST) and cortico-striatal-thalamocortical (CSTC) pathways with probabilistic tractography to assess their (1) integrity and (2) association with motor functioning in people with dyskinetic CP. **Methods:** Diffusion weighted magnetic resonance images were obtained for 33 individuals with dyskinetic CP and 33 controls. Fractional anisotropy (FA) and mean diffusivity (MD) for the CST and the CSTC pathways were compared between groups. Correlation analyses were performed between tensor metric values and motor function scores of participants with dyskinetic CP as assessed by the Gross Motor Function Classification System (GMFCS), the Bimanual Fine Motor Function (BFMF), and the Manual Ability Classification System (MACS). **Results:** White matter integrity in both the CST and the CSTC pathways was reduced in people with dyskinetic CP. The GMFCS, MACS and, less commonly, the BFMF were associated with FA and, particularly, MD in most portions of these pathways. **Interpretation:** The present study advances our understanding of the involvement of white matter microstructure in sensorimotor pathways and its relationship with motor impairment in people with dyskinetic CP. Our results are consistent with well-described relationships between upper limb function and white matter integrity in the CST and CSTC pathways in other forms of CP. This knowledge may ultimately help prognosis and therapeutic programmes.

Introduction

Cerebral palsy (CP) refers to a heterogeneous group of permanent disorders affecting movement, balance, and posture caused by non-progressive disturbances during foetal or early infant brain development.¹ CP is the most frequent cause of physical disability in children and its prevalence is estimated to range from 1 to 3 cases per 1000 live births, depending on several clinical and demographical factors such as the CP type.^{2,3}

There are three CP motor subtypes: spastic, dyskinetic, and ataxic.⁴ The second most common motor type of CP is dyskinetic CP, which is estimated to occur in around 10% of the CP cases.⁵ The core clinical characteristics of dyskinetic CP include abnormal patterns of posture and/or mobility, accompanied by involuntary, uncontrolled, recurrent and, occasionally, stereotyped movements.⁶ The low prevalence of dyskinetic CP and the higher severity of motor impairments compared to other CP subtypes make it difficult to carry out studies of large samples.⁷ There are

few studies on dyskinetic CP available to date, leaving its neuropathological underpinnings incompletely understood.

The different CP subtypes have been traditionally related to different types of observable brain lesions⁸: white matter is frequently impaired in people presenting with spastic CP, while deep grey matter defects are typically observed in dyskinetic CP.⁹ Specifically, the basal ganglia and the thalamus have been commonly identified as the two main brain structures affected in dyskinetic CP, often as the consequence of brief, profound hypoxic insults in term or near-term infants.^{8,10,11} Despite its reputation for deep grey matter damage, around 21% of people with dyskinetic CP appear to present with observable white matter impairment.⁹

Some white matter abnormalities in dyskinetic CP may go unnoticed and therefore be underestimated by qualitative neuroimaging.¹² As 17% of individuals with dyskinetic CP present no visible alterations in conventional neuroimaging⁹ it has been suggested that conventional structural neuroimaging assessments may not be the most optimal predictor of developmental outcomes.¹³ Diffusion-weighted magnetic resonance imaging (DWI) analyses, however, map microstructural characteristics of white matter tracts, allowing more precise correlations with motor function in CP.¹³ Studies performing DWI analyses provide mounting evidence that microstructural white matter abnormalities are present in dyskinetic CP.¹⁴⁻¹⁶ The accurate identification of subtle white matter damage and its association with motor outcomes is of special interest in dyskinetic CP given the involvement of deep grey matter, which plays a key role in the cortico-striatal-thalamocortical (CSTC) pathways responsible for sensorimotor control.¹⁷ That is, deep grey matter damage could result in secondary non-observable abnormalities in the CSTC pathways via retrograde and/or Wallerian degeneration.

Most studies assessing white matter integrity in CP include participants presenting with spastic CP motor type and focus on the corticospinal tract (CST) status.^{12,13} However, the extent to which sensorimotor pathways may be affected in other CP subtypes is less understood. Accordingly, a review highlighted the need to clarify the independent contribution of the different ascending and descending motor and somatosensory tracts in CP, especially in dyskinetic CP.¹⁸ Widespread white matter damage has been described in people presenting with dyskinetic CP through manually drawn regions of interest¹⁹ and voxel-based approaches.¹⁵

Few studies have explored the microstructural integrity of the CST using tractography in people presenting with dyskinetic CP (sample size ranging from 4 to 25 between studies) and results are somewhat inconsistent.^{14,19,20,21} Among these studies, a study from our group¹⁴ examined streamline counts and fractional anisotropy (FA)

measurements from a deterministic whole-brain connectome. Ballester-Plané et al.¹⁴ reported reduced FA in streamlines connecting the precentral gyrus to the brainstem and associations between FA of this tract with gross but not manual motor functioning. Of particular interest, CSTC streamlines connecting the putamen or the thalamus with the precentral or postcentral gyri had lower FA in dyskinetic CP than in controls. Such measurements were associated with gross and manual motor functioning. Limiting further analysis, the cortical parcellation used in this study did not have premotor nor supplementary motor-specific labels, precluding statistical analyses targeting networks including these cortical areas.

As motor training appears to provide a means of restoring impaired motor tract fibres in children with unilateral CP,²² it may be of great value to delineate lesion types and locations for prognosis and to assess and guide novel therapeutic programmes targeting people with dyskinetic CP. To the best of our knowledge, there are no a priori and probabilistic tractography studies precisely delineating the major sensorimotor pathways including both the CST and CSTC pathways in dyskinetic CP.

The current study builds upon a previous exploratory study¹⁴ that examined streamline counts and FA measurements from a deterministic whole-brain connectome. In the current study, we used a partly overlapping but larger sample, and carefully selected the cortical regions of interest to probabilistically delineate those connections involving the premotor cortex and supplementary motor areas. Specifically, the study aims were to (1) assess white matter integrity of sensorimotor pathways including both the CST and the CSTC pathways using DWI; and (2) determine the impact of white matter damage in these pathways on motor functioning. We hypothesise that white matter integrity, determined by FA and mean diffusivity (MD) indexes, will be compromised in all sensorimotor pathways of participants with dyskinetic CP and that these alterations will be linked to their motor impairment.

Methods

Participants

The current study is part of a larger study that focuses on cognitive functioning of people with dyskinetic CP. The current sample overlaps therefore with previously published work. Inclusion criteria for the larger study were (1) clinical diagnosis of CP with predominant dyskinetic features; (2) being older than 6 years; (3) an intelligible yes/no response system; (4) having a minimal comprehension level as evaluated by a raw score ≥ 30 in the Spanish Grammar Screening Test (receptive part).²⁴ This score corresponds to the 10th percentile for 6-year-

old children. Exclusion criteria were the presence of severe visual or auditory disability. Inclusion criteria for the control group were to have the same sex and similar age (± 1 year) as a participant with dyskinetic CP. Controls were ineligible if they were born preterm, were suffering from a neurological or psychiatric disorder, or were illicit substance consumers. Additionally, for the present study, only those participants (CP and controls) who were able to successfully undergo a magnetic resonance imaging (MRI) acquisition session were included. Moreover, when more than three volumes showed substantial motion artefacts during the diffusion preprocessing and modelling the participant was excluded entirely from further analysis.

All procedures performed in the study were in accordance with the ethical standards of the 1964 Helsinki declaration and its later amendments or comparable ethical standards. Ethical approval was obtained by the Bioethics Commission of the University of Barcelona, Institutional Review Board (IRB 00003099, assurance number: FWA00004225; <http://www.ub.edu.sire.ub.edu/recerca/comissiobioetica.htm>), and the Vall d'Hebron University Hospital. Written informed consents were obtained from all participants or their legal guardian.

Motor assessment

Gross motor functioning was assessed by the Gross Motor Function Classification System (GMFCS),^{25,26} which classifies individuals with CP on the basis of functional abilities and limitations. Bimanual functioning was assessed by the Bimanual Fine Motor Function (BFMF)²⁷ and manual ability, by the Manual Ability Classification System (MACS).²⁸ The three scales each contain five levels of classification, higher scores indicating poorer motor functioning (from level I to V).

Neuroimaging

Image acquisition

MRI data were acquired on a Siemens Magnetom TRIO 3-Tesla scanner (Erlangen, Germany; 45 mT/m, slew rate 200 T/m/s), with 12-channel head coil at the Vall d'Hebron University Hospital (Barcelona, Spain).

Diffusion weighted images were acquired in 30 noncollinear directions at $b = 1000$ s/mm², plus one minimally diffusion weighted image ($b = 0$). Acquisition parameters were 2 mm slice thickness; 65 axial slices; field of view 240 × 240 mm; TR/TE 8400/90 ms; TA 4:47 min; acquisition matrix 122 × 122, voxel size 1.96 × 1.96 mm.

To minimise movement during data acquisition, diazepam was administered to 13 participants (dose

between 2.5 and 10 mg, depending on each participant) and 6 were sedated with pentobarbital and propofol. The drug was prescribed by a physician in accordance with the protocol detailed and approved by the ethics committee.

Diffusion preprocessing and modelling

The HARDI DWI pipeline used has been published in detail elsewhere.^{29,30} In brief, DWI data underwent extensive preprocessing, including correction for image artefacts caused by image distortions, cardiac pulsation, and head motion. Volumes were excluded from further analyses when containing within-volume motion or scanner artefacts; when more than three volumes showed substantial motion artefacts the participant was excluded entirely from further analysis. MRtrix3 was then used to calculate tensor metrics across the whole-brain and to estimate fibre orientation distributions for tractography using constrained spherical deconvolution.³¹

Atlases

A study-specific atlas was generated by co-registering FA images of all participants using ANTS-SyN,³² after which non-linear transforms were calculated from FA maps of all participants to this finalised atlas, as detailed in Laporta-Hoyos *et al.*¹⁵ The Harvard-Oxford cortical and subcortical structural atlases (Makris *et al.*,³³; Frazier *et al.*,³⁴; Desikan *et al.*,³⁵; Goldstein *et al.*,³⁶) and the Jülich histological (cyto- and myelo-architectonic) atlases³⁷⁻³⁹ were used to select cortical and deep grey matter regions of interest for later use in tractography (Table 1). To enable this, these atlases were non-linearly registered to the study-specific template using ANTs and their labels subsequently transformed into each subject's native diffusion space.

Table 1. Atlases labels comprising the cortical regions of interest.

ROI names	Harvard-Oxford cortical structural atlases labels unless otherwise indicated in italics
Precentral gyrus	Precentral gyrus
Postcentral gyrus	Postcentral gyrus
Premotor and supplementary motor cortices	GM premotor cortex BA6 (<i>Jülich histological atlas</i>), which comprises the juxtapositional lobule cortex (formerly supplementary motor cortex) The portions of the ROI that extended to the precentral and postcentral ROI areas were removed

BA, Brodmann area; GM, grey matter; ROI, regions of interest.

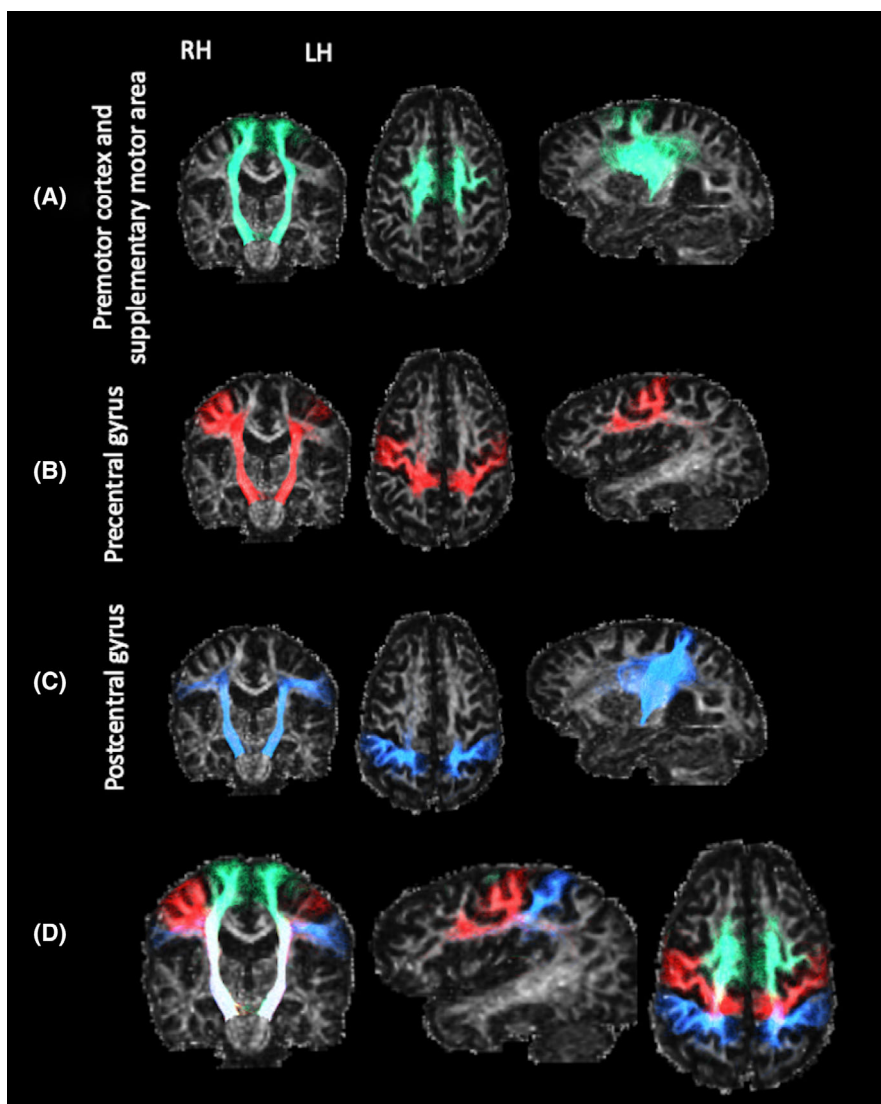


Figure 1. Example of the generated tractography for the corticospinal tract. Streamlines targeting (A) the premotor and supplementary motor areas, (B) the precentral gyrus, and (C) the postcentral gyrus are presented. The last column (D) presents all streamlines together (A + B + C). Sagittal slices show the right hemisphere. The sagittal slice shown differs between rows to best demonstrate the tractography. LH, left hemisphere; RH, right hemisphere.

Tractography

For each of the following tracts, streamline generation was performed using MRtrix3's iFOD2 algorithm until microstructural sample reliability stability criteria were met (minimum streamline count 3000, target standard deviations: FA, 0.001; MD, 1×10^{-6}).⁴⁰ Tracts were delineated separately for each hemisphere and mean FA and MD were calculated for each pathway. Means for left and right hemispheres were then averaged to arrive at a single FA or MD measurement per participant pathway.

Three CST pathways were delineated per hemisphere (Fig. 1). These were generated by seeding streamlines

from the brainstem and filtered to include only those passing through the posterior limb of the internal capsule and terminating in either (1) the premotor or supplementary motor areas (i.e., Brodmann area 6), (2) the precentral gyrus, or (3) the postcentral gyrus. To prevent including streamlines that are part of the CSTC pathways, those streamlines traversing the basal ganglia, the thalamus or being part of the corpus callosum were excluded.

Nine CSTC pathways involved in sensorimotor control were delineated per hemisphere (Fig. 2). Each tract was seeded from one of the caudate, putamen or thalamus, and terminated in either (1) the premotor and supplementary motor areas, (2) the precentral gyrus, or (3) the

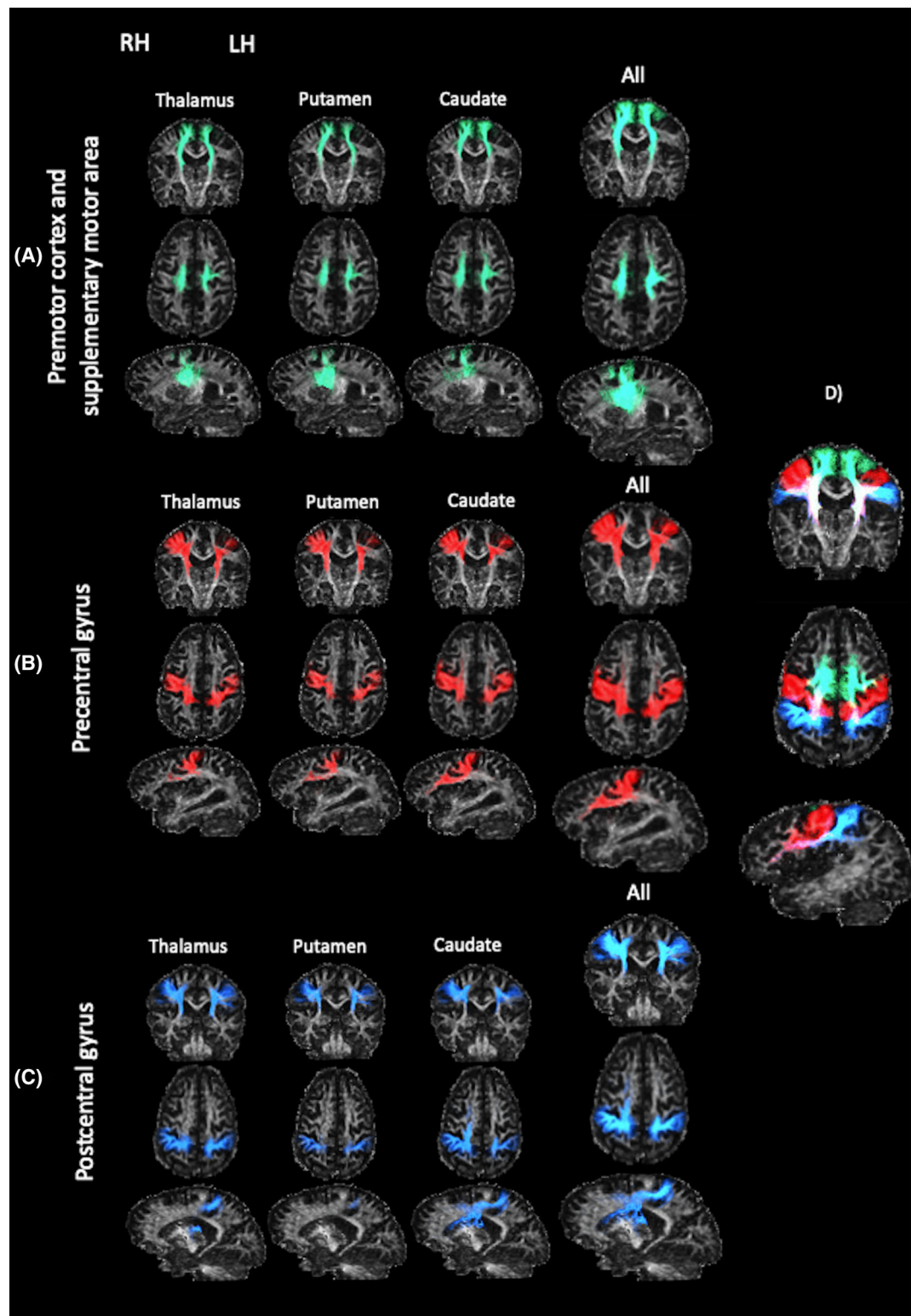


Figure 2. Example of the generated tractography for the cortico-striatal-thalamocortical pathways involved in sensorimotor control targeting (A) the premotor and supplementary motor areas, (B) the precentral gyrus, and (C) the postcentral gyrus. Streamlines seeding from the thalamus, the putamen and the caudate are presented separately and altogether (column “all”). The last column (D) presents all streamlines together (A + B + C). Sagittal slices show the right hemisphere. LH, left hemisphere; RH, right hemisphere.

postcentral gyrus. Several exclusion regions were applied to avoid anatomically implausible streamlines.

The pathway connecting the caudate nucleus with the prefrontal cortex was used as a negative control, due to the relatively prominent involvement of the caudate nucleus in cognitive function.⁴¹ The tract was delineated by seeding from the caudate nucleus, passing through the anterior limb of the internal capsule, and terminating in any cortical grey matter within the prefrontal cortex.

To exclude streamlines entering a non-target grey matter region, an exclusion mask was generated for each subject by identifying voxels outside of the seed regions where FA <0.2 and eroding by one voxel. All tractography was visually checked and mean FA and MD were calculated for each pathway using MRtrix's tcksample.

Statistical analysis

FA and MD in the assessed tracts were compared between people with dyskinetic CP and the control group using standardised mean difference for independent samples (equivalent to Student's *t*) and *p*-values were approximated using permutation tests based on 1000 resamples. Absolute Cohen's *d* values between 0.5 and 0.8 or greater were considered medium and large effect sizes, respectively.⁴²

Kendall's correlations were carried out to explore the association between FA and MD in the assessed tracts and gross and manual motor functioning (i.e., GMFCS, BFMF, and MACS). The 95% confidence intervals were obtained for all pairwise relationships based on a BCa-Bootstrapping with 1000 replications. Additionally, effect size was also interpreted by inspecting absolute correlation values, considering the effects as small when $r_{\tau} \geq 0.1$, medium if $r_{\tau} \geq 0.3$, and large when $r_{\tau} \geq 0.5$.⁴² The significance level was set at 0.05 and data were analysed with R software (v. 4.2.1).

FA and MD indices assess different aspects of white matter microstructure: MD the absolute average diffusivity and FA a unitless ratio of diffusivity of the major fibre orientation relative to its orthogonal directions. Therefore, each performed test targets a different hypothesis. Results after applying multiple comparisons correction are not presented in the manuscript but are available as Supporting Information (Tables S1 and S2).

The possible confounding effect of age was evaluated by repeating our correlation analyses with age as an additional covariate.

Results

Group characteristics

This cross-sectional observational study included 33 participants with dyskinetic CP aged 6–59 years (15 females)

who satisfied the general inclusion criteria and were able to successfully undergo an MRI acquisition session. Thirty-three typically developing healthy controls matched by age and sex were also included. FA and MD values and motor scores for both groups were determined (Table 2). Further details about the clinical characteristics of the sample are described elsewhere.¹⁵

Integrity of sensorimotor pathways

Comparisons of FA and MD values between participants presenting with dyskinetic CP and controls were performed (Table 3).

CST

People presenting with dyskinetic CP showed lower FA values compared to controls in all tracts assessed, with medium to large effect sizes (Cohen's *d* ranging from -0.7 to -0.8). Consistently, people presenting with dyskinetic CP showed higher MD values in all tracts assessed, with large effect sizes (Cohen's *d* ranging from 1.0 to 1.3).

CSTC pathways

People presenting with dyskinetic CP showed lower FA values compared to controls in tracts seeding from the caudate and targeting premotor and supplementary motor areas as well as in tracts seeding from the caudate, the putamen and the thalamus and targeting the precentral and the postcentral gyri, with medium to large effect sizes (Cohen's *d* ranging from -0.6 to -0.8). Regarding MD, people presenting with dyskinetic CP showed higher values compared to controls in all tracts assessed, with large effect sizes (Cohen's *d* ranging from 1.0 to 1.4).

No relationship was found between diffusion tensor metrics of the tract connecting the caudate nucleus with the prefrontal cortex and any of the motor function scale scores.

Relationship between sensorimotor pathways and motor functioning

Correlations between FA and MD values and motor functioning were performed (Table 4, Fig. 3).

CST

GMFCS scores negatively correlated with mean tract FA values for white matter tracts connecting the brainstem with the premotor and the supplementary motor areas and with the precentral gyrus, with medium ($r_{\tau} = -0.3$)

Table 2. Descriptive statistics for tensor metrics values and motor functioning of the dyskinetic cerebral palsy and control groups.

	Dyskinetic CP (n = 33)	Control (n = 33)
Fractional anisotropy, mean (SD)		
PreM and SuppM to brainstem	0.55 (0.03)	0.57 (0.02)
PreCG to brainstem	0.55 (0.03)	0.57 (0.03)
PostCG to brainstem	0.53 (0.03)	0.55 (0.03)
Caudate to PreM and SuppM	0.43 (0.04)	0.45 (0.02)
Putamen to PreM and SuppM	0.46 (0.03)	0.48 (0.02)
Thalamus to PreM and SuppM	0.49 (0.04)	0.50 (0.02)
Caudate to PreCG	0.40 (0.03)	0.42 (0.02)
Putamen to PreCG	0.45 (0.04)	0.47 (0.03)
Thalamus to PreCG	0.47 (0.04)	0.49 (0.03)
Caudate to PostCG	0.40 (0.03)	0.42 (0.03)
Putamen to PostCG	0.45 (0.03)	0.48 (0.03)
Thalamus to PostCG	0.45 (0.04)	0.47 (0.03)
Mean diffusivity, mean (SD)		
PreM and SuppM to brainstem	0.79 × 10 ⁻³ (0.049 × 10 ⁻³)	0.75 × 10 ⁻³ (0.025 × 10 ⁻³)
PreCG to brainstem	0.81 × 10 ⁻³ (0.055 × 10 ⁻³)	0.76 × 10 ⁻³ (0.024 × 10 ⁻³)
PostCG to brainstem	0.83 × 10 ⁻³ (0.049 × 10 ⁻³)	0.78 × 10 ⁻³ (0.025 × 10 ⁻³)
Caudate to PreM and SuppM	0.83 × 10 ⁻³ (0.066 × 10 ⁻³)	0.77 × 10 ⁻³ (0.033 × 10 ⁻³)
Putamen to PreM and SuppM	0.78 × 10 ⁻³ (0.061 × 10 ⁻³)	0.73 × 10 ⁻³ (0.028 × 10 ⁻³)
Thalamus to PreM and SuppM	0.78 × 10 ⁻³ (0.074 × 10 ⁻³)	0.72 × 10 ⁻³ (0.027 × 10 ⁻³)
Caudate to PreCG	0.83 × 10 ⁻³ (0.073 × 10 ⁻³)	0.76 × 10 ⁻³ (0.030 × 10 ⁻³)
Putamen to PreCG	0.79 × 10 ⁻³ (0.065 × 10 ⁻³)	0.73 × 10 ⁻³ (0.025 × 10 ⁻³)
Thalamus to PreCG	0.81 × 10 ⁻³ (0.084 × 10 ⁻³)	0.73 × 10 ⁻³ (0.023 × 10 ⁻³)
Caudate to PostCG	0.87 × 10 ⁻³ (0.076 × 10 ⁻³)	0.80 × 10 ⁻³ (0.032 × 10 ⁻³)
Putamen to PostCG	0.80 × 10 ⁻³ (0.051 × 10 ⁻³)	0.75 × 10 ⁻³ (0.024 × 10 ⁻³)
Thalamus to PostCG	0.84 × 10 ⁻³ (0.073 × 10 ⁻³)	0.77 × 10 ⁻³ (0.027 × 10 ⁻³)
Motor outcomes (n)		
GMFCS	I (12); II (6); III (3); IV (5); V (7)	
BFMF	I (6); II (9); III (8); IV (6); V (4)	
MACS	I (5); II (8); III (11); IV (2); V (7)	

BFMF, Bimanual Fine Motor Function; CP, cerebral palsy; GMFCS, Gross Motor Function Classification System; MACS, Manual Ability Classification System; PreM, premotor area; PostCG, postcentral gyrus; PreCG, precentral gyrus; SD, standard deviation; SuppM, supplementary motor area.

effect sizes. GMFCS scores did not correlate with FA values of equivalent tracts entering the postcentral gyrus. MACS scores were negatively correlated with FA values in

all the tracts assessed, with medium effect sizes (r_τ ranging from -0.3 to -0.4). GMFCS scores were positively correlated with MD values in all tracts assessed, with medium effect sizes (r_τ ranging from 0.3 to 0.4). MACS scores were positively correlated with tracts connecting the brainstem with the precentral gyrus ($r_\tau = 0.3$) and the postcentral gyrus ($r_\tau = 0.4$), with medium effect sizes, but not with those terminating in the premotor nor the supplementary motor areas. BFMF scores were not significantly associated with FA nor MD in any tract.

CSTC pathways

GMFCS scores were negatively correlated with mean FA values of tracts connecting the caudate with the premotor and the supplementary motor areas and with the precentral and postcentral gyri, with medium effect sizes (r_τ ranging from -0.3 to -0.4). GMFCS scores were also significantly associated with mean FA values of tracts connecting the putamen with the precentral gyrus, with medium effect sizes ($r_\tau = -0.3$).

BFMF and MACS scores were negatively correlated with mean tract FA of white matter tracts connecting the caudate and the putamen with the precentral gyrus and the caudate with the postcentral gyrus. MACS scores, additionally, were negatively correlated with FA values of tracts connecting the caudate to premotor and supplementary motor areas, the thalamus with the precentral and postcentral gyri, and the putamen with the postcentral gyrus. These correlations showed medium to large effect sizes (r_τ ranging from -0.3 to -0.5).

Scores in the GMFCS were positively correlated with mean MD values of all the tracts assessed, with medium to large effect sizes (r_τ ranging from 0.3 to 0.5). BFMF scores were positively correlated with MD values in the tracts connecting the caudate and the thalamus with the postcentral gyrus, with medium effect sizes ($r_\tau = 0.3$). MACS scores were positively correlated with MD of all tracts assessed but the ones connecting the putamen with the premotor and supplementary motor areas. These correlations showed medium to large effect sizes (r_τ ranging from 0.3 to 0.5).

There were no changes as to which associations reached statistical significance for the correlation analyses with age as additional covariate (Table S3).

Discussion

In the current study we performed a priori and probabilistic tractography precisely delineating microstructural measurements of the CST and CSTC sensorimotor pathways in dyskinetic CP. We also explored whether microstructural alterations in these pathways, considering both

Table 3. Comparison of fractional anisotropy and mean diffusivity values between participants presenting with dyskinetic cerebral palsy and controls.

	Fractional anisotropy			Mean diffusivity		
	<i>t</i>	95% CI mean difference	Cohen's <i>d</i>	<i>t</i>	95% CI mean difference	Cohen's <i>d</i>
Corticospinal tract						
PreM and SuppM to brainstem	-2.5*	-0.03, -0.004	-0.7	3.6***	1.9×10^{-5} , 5.9×10^{-5}	1.0
PreCG to brainstem	-3.1**	-0.04, -0.01	-0.8	4.1***	2.8×10^{-5} , 7.0×10^{-5}	1.1
PostCG to brainstem	-3.2***	-0.04, -0.01	-0.8	4.3***	2.9×10^{-5} , 6.7×10^{-5}	1.3
Cortico-striatal-thalamocortical pathways						
Caudate to PreM and SuppM	-2.6**	-0.04, -0.01	-0.7	3.9***	3.2×10^{-5} , 8.4×10^{-5}	1.1
Putamen to PreM and SuppM	-1.8	-0.03, 0.001	-0.5	3.7***	2.5×10^{-5} , 7.2×10^{-5}	1.0
Thalamus to PreM and SuppM	-1.3	-0.03, 0.01	-0.3	3.8***	3.1×10^{-5} , 8.7×10^{-5}	1.1
Caudate to PreCG	-3.1***	-0.04, -0.01	-0.8	4.2***	3.9×10^{-5} , 9.5×10^{-5}	1.2
Putamen to PreCG	-2.8**	-0.04, -0.01	-0.7	4.0***	3.1×10^{-5} , 8.0×10^{-5}	1.1
Thalamus to PreCG	-2.4*	-0.04, -0.004	-0.6	4.2***	4.4×10^{-5} , 1.1×10^{-4}	1.2
Caudate to PostCG	-3.2***	-0.04, -0.01	-0.8	4.0***	3.8×10^{-5} , 9.6×10^{-5}	1.1
Putamen to PostCG	-3.1**	-0.04, -0.01	-0.8	4.3***	3.0×10^{-5} , 7.0×10^{-5}	1.3
Thalamus to PostCG	-2.7**	-0.04, -0.01	-0.7	4.6***	4.8×10^{-5} , 1.0×10^{-4}	1.4

CI, confidence interval; PreM, premotor area; PostCG, postcentral gyrus; PreCG, precentral gyrus; SD, standard deviation; SuppM, supplementary motor area.

* $p < 0.05$;

** $p < 0.01$;

*** $p < 0.001$.

FA and MD, are associated with gross motor functioning and manual ability.

Results indicate that FA and, particularly, MD in sensorimotor pathways are impaired in dyskinetic CP and associated with GMFCS, MACS and, less commonly, BFMF. Specifically, we found that people with dyskinetic CP present with lower FA and increased MD in comparison to controls in all the CST branches assessed. The results of the present study align with those previously reported by our group in partly¹⁴ or fully¹⁵ overlapping samples, ratifying the presence of microstructural axonal abnormalities in the CST of participants presenting with dyskinetic CP. Our current results expand beyond Ballester-Plané et al.¹⁴ as here we found not only reduced FA in those streamlines connecting the brainstem with the precentral gyrus but also in streamlines connecting with the postcentral gyrus and the premotor and supplementary motor areas.

The integrity of the CST in dyskinetic CP was also assessed using tractography in two previous studies from other groups.^{20,21} Harlaar et al.²⁰ reported reduced CST volume but no FA reductions in a small sample of people presenting with dyskinetic CP that also included a participant with spastic CP ($n = 5$). Similarly, Park et al.²¹ reported no differences in the number of CST fibres and FA values between people with dyskinetic CP and the control group in a sample of 23 participants. Our FA results, observed in a larger sample including adults, are consistent with the findings of Yoshida et al.¹⁹ ($n = 19$) in children, who manually defined regions of interest in

the CST at the pons, the anterior limb of the internal capsule, and the posterior limb of the internal capsule and found reduced FA in participants presenting with dyskinetic CP compared to controls and increased MD in all regions but the CST at the pons. Notably, we obtained more consistent results with MD than FA, but MD has been infrequently reported in previous works, limiting our ability to make direct comparisons. These studies' remaining discrepancies regarding the involvement of the CST may be due to some studies' small sample sizes, focuses on different aspects of the descending motor pathways, or utilisation of substantially different tractographic approaches such as deterministic whole-brain versus targeted probabilistic tractography. Additionally, the degree in which features of spasticity may be present in different samples may also explain differences between studies. Alterations in the CST have been traditionally related to spastic CP¹² but dyskinetic CP may be accompanied by comorbid spastic symptomatology.^{43,44} Future studies objectively measuring such symptoms could allow to disentangle whether CST alterations observed in dyskinetic CP are associated with the comorbid symptoms of spasticity. Regarding the sensorimotor CSTC pathways, we found they presented with increased MD and decreased FA in all branches except for those connecting the premotor and supplementary motor areas with the putamen and the thalamus. The CSTC pathways connect brain structures typically involved in dyskinetic CP, namely, the basal ganglia and the thalamus, with

Table 4. Kendall's correlation coefficients for the associations between fractional anisotropy and mean diffusivity values and functional motor outcomes.

	Fractional anisotropy			Mean diffusivity		
	GMFCS	BFMF	MACS	GMFCS	BFMF	MACS
Corticospinal tract						
PreM and SuppM to brainstem	-0.28* (-0.5; 0.1)	-0.19 (-0.5; 0.1)	-0.28* (-0.5; 0.6)	0.29* (-0.03; 0.06)	0.09 (-0.2; 0.4)	0.23 (-0.1; 0.5)
PreCG to brainstem	-0.32* (-0.56; -0.002)	-0.23 (-0.47; 0.082)	-0.35** (-0.6; 0.016)	0.36** (0.1; 0.6)	0.13 (-0.2; 0.4)	0.29* (-0.1; 0.5)
PostCG to brainstem	-0.24 (-0.5; 0.1)	-0.18 (-0.4; 0.1)	-0.30* (-0.6; 0.04)	0.42** (0.1; 0.6)	0.19 (-0.2; 0.5)	0.35** (0.007; 0.6)
Cortico-striatal-thalamo-cortical pathways						
Caudate to PreM and SuppM	-0.32* (-0.6; -0.02)	-0.24 (-0.5; 0.1)	-0.32* (-0.6; 0.04)	0.39** (0.1; 0.6)	0.19 (-0.1; 0.4)	0.33* (-0.002; 0.6)
Putamen to PreM and SuppM	-0.19 (-0.5; 0.1)	-0.16 (-0.5; 0.2)	-0.23 (-0.5; 0.2)	0.30* (-0.1; 0.6)	0.11 (-0.2; 0.4)	0.24 (-0.1; 0.5)
Thalamus to PreM and SuppM	-0.17 (-0.5; 0.1)	-0.21 (-0.5; 0.1)	-0.24 (-0.5; 0.1)	0.35** (0.01; 0.6)	0.13 (-0.2; 0.4)	0.28* (-0.03; 0.6)
Caudate to PreCG	-0.39** (-0.6; -0.1)	-0.34** (-0.6; -0.004)	-0.45** (-0.7; -0.1)	0.46** (0.2; 0.7)	0.25 (-0.1; 0.5)	0.41** (0.1; 0.6)
Putamen to PreCG	-0.31* (-0.5; 0.01)	-0.30* (-0.5; 0.04)	-0.39** (-0.6; -0.04)	0.47** (0.2; 0.7)	0.26 (-0.1; 0.5)	0.40** (0.05; 0.6)
Thalamus to PreCG	-0.17 (-0.5; 0.1)	-0.26 (-0.5; 0.05)	-0.29* (-0.5; 0.1)	0.44** (0.1; 0.6)	0.23 (-0.1; 0.5)	0.39** (0.1; 0.6)
Caudate to PostCG	-0.32* (-0.5; 0.002)	-0.27* (-0.5; 0.1)	-0.36** (-0.6; -0.02)	0.50*** (0.2; 0.7)	0.26* (-0.1; 0.5)	0.40** (0.1; 0.6)
Putamen to PostCG	-0.20 (-0.5; 0.1)	-0.22 (-0.5; 0.1)	-0.28* (-0.5; 0.1)	0.44** (0.1; 0.7)	0.26 (-0.1; 0.5)	0.41** (0.1; 0.7)
Thalamus to PostCG	-0.18 (-0.5; 0.1)	-0.23 (-0.5; 0.1)	-0.28* (-0.5; 0.03)	0.48** (0.2; 0.7)	0.28* (-0.1; 0.5)	0.45*** (0.1; 0.7)

95% BCa-Bootstrap confidence intervals are shown within brackets.

BFMF, Bimanual Fine motor function; GMFCS, Gross Motor Function Classification System; MACS, Manual Ability Classification System.

* $p < 0.05$;

** $p < 0.01$;

*** $p < 0.001$.

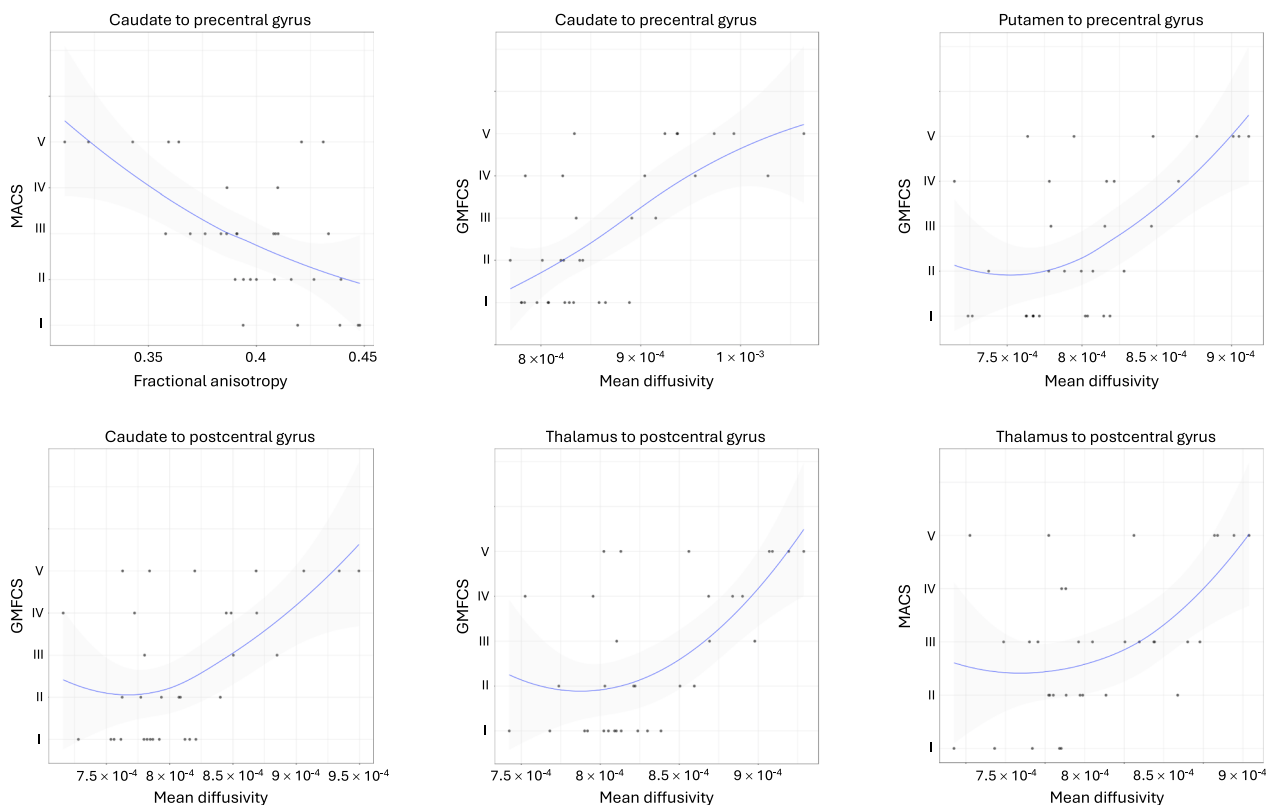


Figure 3. Correlations between diffusion tensor metrics and gross motor function. Only tracts showing differences between groups and large correlations with motor functioning scores are shown.

sensorimotor cortical regions, such as the premotor, the primary motor, and the primary somatosensory cortices. These connections are involved in precision, timing, compensatory muscle tone, and balance, among other features of motor control.⁴⁵⁻⁴⁸ Our results are mostly consistent with the only previous tractography study that used a deterministic whole-brain connectome approach in people presenting with dyskinetic CP¹⁴ but some discrepancies should be noted, such as that in the current study white matter damage was identified in different tracts of the CSTC pathways including the premotor and supplementary motor areas, but the same was not specifically explored in Ballester-Plané *et al.*¹⁴

We found significant associations between the CST tensor metrics and both GMFCS and MACS but not BFMF. Poorer GMFCS, MACS, and BFMF severity classifications were also associated with reduced white matter integrity in many aspects of the sensorimotor CSTC pathways. The BFMF, however, was less frequently associated with white matter integrity in these pathways. Again, our results are partly consistent with Ballester-Plané *et al.*¹⁴ as both studies identified associations between the CST (precentral

gyrus to brainstem) and the GMFCS as well as the CSTC pathways and both the GMFCS and the MACS. The results of the present study, however, identify additional associations, including associations between both (1) GMFCS levels with the integrity in other branches of the CST (postcentral gyrus, premotor and supplementary motor areas to brainstem); and (2) MACS levels with the integrity of the CST. Of note, for all the aforementioned discrepancies, statistical analyses of premotor and supplementary motor areas were not possible in Ballester-Plané *et al.*¹⁴ due to the parcellation scheme used, while the remaining discrepancies are likely driven by the different degree of sensitivity between methodological approaches.

Correlations reported here between the GMFCS/MACS and the CSTC pathway tensor metrics dovetail with previously reported associations between the GMFCS/MACS and dystonic symptomatology.⁴⁹ These also align with the tendency for children with dyskinetic CP to present with similar levels of gross motor function and manual ability.⁵⁰ The present results are also consistent with well described relationships between upper limb function and white matter integrity in the CST and CSTC pathways in

other forms of CP, particularly unilateral spastic CP.^{18,51} The lack of association between the MACS and the CST white matter integrity in Ballester-Plané *et al.*¹⁴ and the fact that in the present study the BFMF was not associated with the CST white matter integrity but that these associations were found with the CSTC pathways are consistent with the hypothesis that somatosensation could be a critical driver of hand function in unilateral spastic CP, over the CST status.⁵²

The BFMF was not associated with the CST tensor metrics and was less frequently associated with metrics in the CSTC tracts than MACS categories. The less frequent associations of BFMF than MACS categories with the status of sensorimotor pathways could be due to the fact that these two classification systems measure different aspects of functioning. While the MACS classifies children's manual capacity in daily life irrespective of differences between the two hands, the BFMF scale assesses fine motor function in each hand separately.²⁷ These differences could explain, at least partially, why only the MACS appeared to be sensitive to white matter loss of integrity.

While FA and MD results are mostly consistent for all explored tracts and analyses, there were two tracts where MD, but not FA, was reduced in dyskinetic CP participants compared to controls. Significant differences on these pathways' tensor metrics between people with dyskinetic CP and controls also show greater effect sizes for MD than FA. Similarly, seven significant associations between MD, but not FA, values and motor functioning scores were found. It is likely that this reflects the strengths and limitations of these measures. That is, while FA measures may be more sensitive than MD in voxels containing only a single fibre direction, its validity is reduced where fibres cross and/or fan.⁵³ MD is likely a more ideal measure for the present study due to our focus on tracts that are dominated by branching, fanning, and/or contain crossing fibres from other white matter tracts.

Some limitations necessitate interpreting the present results carefully. To our knowledge, the present work is the largest study so far exploring the sensorimotor pathways in people with dyskinetic CP but is nevertheless limited by its moderate sample size. Another limitation is the inclusion criterion of having minimal verbal comprehension so our results may not extrapolate to those cases without or with very basic verbal comprehension. This inclusion criterion was set since the current study is part of a larger one targeting cognition in dyskinetic CP. Despite this being a limitation, the sample is still relatively representative of people with dyskinetic CP, and only three participants were not included due to such inclusion criterion. Third, our sample includes

participants with a broad age range and we aimed to minimise age effects by age-matching participants with CP and controls. Such age matching, however, could be undermined by white matter injury disrupting the normal white matter maturational process⁵⁴ in participants with CP. While our sample characteristics did not allow us to deeply analyse age effects, when we evaluated this possible confound by repeating our correlation analyses with age as an additional covariate there were no changes as to which associations reached statistical significance (Table S3). Thus, although it would be interesting to specifically evaluate how the relationship between diffusion tensor metrics and motor function is affected by age, it appears that matching of controls by age was sufficient for the goals of the present study. Another limitation was that tract delineation was driven by anatomical landmarks. It is possible that, because of the brain lesion and resulting plasticity processes, the actual location of the functional areas of the brain is altered in our participants, as it has already been shown in other types of CP.^{55,56} To address this issue, some studies have used functional neuroimaging methods, such as magnetoencephalography and functional MRI to guide diffusion analyses.⁵⁵⁻⁵⁷ However, functional data were not available for our participants. Our own experience suggests such approaches can meaningfully improve tractography specificity and statistical power^{58,59} but bring additional challenges including higher risk of partial data loss and controlling for task difficulty in functionally heterogeneous cohorts. Another limitation may be the lack of other diffusivity measures, such as axial (AD) and radial diffusivity (RD). Although AD and RD may be interesting and potentially useful supplementary metrics, we did not include them in our analysis. There were two main factors that discouraged us from analysing AD and RD. One is that FA and MD are strongly correlated with AD and RD. Thus, additional hypotheses for RD and AD would provide only modest new insight while adding a need for stringent multiple comparisons correction and a corresponding decrease in statistical power. The second factor is the reliability of these measures when they are obtained from voxels containing multiple fibre populations with different orientations.⁶⁰ Although AD and RD may provide reliable results in healthy subjects and in certain pathological conditions, some authors advise against the use of these parameters in conditions associated with altered myelination or where pathology has otherwise caused a decrease in anisotropy.^{61,62} Finally, we opted for an a priori, targeted, rather than for a whole-brain approach. Whole-brain approaches are primarily useful for exploratory work, when no specific testable hypotheses regarding the relationship between brain and function can be made. Besides, the large amount of statistical comparisons

associated to whole-brain analyses requires large sample sizes, which are challenging to achieve in certain conditions, such as dyskinetic CP. As we had specific hypotheses which we wanted to test and a limited sample size, we selected a targeted approach to test those – and only those – hypotheses.

Future research is warranted to not only overcome the aforementioned limitations of the present work, but also to advance in the characterisation of the neural substrate of dyskinetic CP. One first line of research could be aimed at identifying the specific neural characteristics of dyskinetic CP patients presenting with predominantly choreoathetotic versus predominantly dystonic symptomatology. Another future line of research could be focused on the examination of motor tracts controlling lower limbs and trunk, which are also affected in dyskinetic CP. In this sense, the use of the recently created Dyskinesia Impairment Scale⁶³ would be of great value for these two purposes, as it allows the evaluation of dystonia and choreoathetosis both in action and rest in up to 11 body regions, including lower and upper limbs, and trunk. Finally, as CP is not only characterised by motor impairment, but also by cognitive affectation, determining the neural substrates of the cognitive deficits present in dyskinetic CP would also be a promising line of research. Such efforts to thoroughly characterise different phenotypes of dyskinetic CP should be of great value for the advance of therapeutic approaches, such as deep brain stimulation, whose targeting could profit the precise identification of the primarily affected brain networks.

In conclusion, tractography analyses indicate white matter integrity – as measured by FA and, particularly, MD – is reduced in the CST and CSTC sensorimotor pathways in dyskinetic CP. Although it is important to remember that correlations do not involve causal relationships, the white matter integrity of these pathways showed consistent associations with the GMFCS and the MACS, while associations with the BFMF were constrained to only a few branches of the CSTC sensorimotor pathways. The present study also highlights how different tractography approaches can have clearly different strengths when it comes to identifying white matter integrity, something that should be considered when developing technology to translate neuroimaging analyses into clinical practice.

Acknowledgments

This work was supported by the Ministerio de Ciencia e Innovación (PSI2011/24386), and by the Agencia Estatal de Investigación (PID2020-117163RB-I00/AEI/10.13039/501100011033). Olga Laporta-Hoyos received a research grant from Ministerio de Educación, Cultura y Deporte

of the Government of Spain (FPU13/06435). This project was supported by National Health and Medical Research Council of Australia (1037220). The authors wish to thank all participants and their families for their collaboration.

Conflict of Interest

The authors declare no conflicts of interest.

Author Contributions

Writing – original draft preparation: Xavier Caldú; Investigation: Xavier Caldú, Júlia Ballester-Plané, and Olga Laporta-Hoyos; Methodology: Lee B. Reid, Kerstin Pannek, Jurgen Fripp, and David Leiva; Formal analysis: Lee B Reid, Kerstin Pannek, Jurgen Fripp, David Leiva, and Olga Laporta-Hoyos; Funding acquisition: Roslyn N. Boyd, Roser Pueyo, and Olga Laporta-Hoyos; Conceptualisation: Roser Pueyo and Olga Laporta-Hoyos; Project administration: Roser Pueyo; Supervision: Roser Pueyo; Data curation: Roser Pueyo; Writing – review and editing: Xavier Caldú, Lee B. Reid, Kerstin Pannek, Jurgen Fripp, Júlia Ballester-Plané, David Leiva, Roslyn N. Boyd, Roser Pueyo, and Olga Laporta-Hoyos.

Data Availability Statement

The data that support the findings of this study are available from the corresponding author upon reasonable request.

References

- Rosenbaum P, Paneth N, Leviton A, et al. A report: the definition and classification of cerebral palsy April 2006. *Dev Med Child Neurol.* 2007;49(SUPPL. 2):8-14.
- Galea C, McIntyre S, Smithers-Sheedy H, et al. Cerebral palsy trends in Australia (1995-2009): a population-based observational study. *Dev Med Child Neurol.* 2019;61(2):186-193.
- Sellier E, Platt MJ, Andersen GL, et al. Decreasing prevalence in cerebral palsy: a multi-site European population-based study, 1980 to 2003. *Dev Med Child Neurol.* 2016;58(1):85-92.
- Cans C. Surveillance of cerebral palsy in Europe: a collaboration of cerebral palsy surveys and registers. Surveillance of cerebral palsy in Europe (SCPE). *Dev Med Child Neurol.* 2000;42(12):816-824.
- Himmelman K, McManus V, Hagberg G, et al. Dyskinetic cerebral palsy in Europe: trends in prevalence and severity. *Arch Dis Child.* 2009;94(12):921-926.
- Cans C, Dolk H, Platt MJ, et al. Recommendations from the SCPE collaborative group for defining and classifying

- cerebral palsy. *Dev Med Child Neurol Suppl.* 2007;109 (SUPPL. 2):35-38.
7. Pueyo R. Towards a comprehensive profile of dyskinetic cerebral palsy. *Dev Med Child Neurol.* 2017;59(6):570.
 8. Krägeloh-Mann I, Cans C. Cerebral palsy update. *Brain and Development.* 2009;31(7):537-544.
 9. Horber V, Sellier E, Horridge K, et al. The origin of the cerebral palsies: contribution of population-based neuroimaging data. *Neuropediatrics.* 2020;51(2):113-119.
 10. Himmelmann K, Uvebrant P. Function and neuroimaging in cerebral palsy: a population-based study. *Dev Med Child Neurol.* 2011;53(6):516-521.
 11. Yokochi K, Aiba K, Kodama M, Fujimoto S. Magnetic resonance imaging in athetotic cerebral palsied children. *Acta Paediatr Scand.* 1991;80(8-9):818-823.
 12. Scheck SM, Boyd RN, Rose SE. New insights into the pathology of white matter tracts in cerebral palsy from diffusion magnetic resonance imaging: a systematic review. *Dev Med Child Neurol.* 2012;54(8):684-696.
 13. Franki I, Maillieux L, Emsell L, et al. The relationship between neuroimaging and motor outcome in children with cerebral palsy: a systematic review - part a. structural imaging. *Res Dev Disabil.* 2020;100:100.
 14. Ballester-Plané J, Schmidt R, Laporta-Hoyos O, et al. Whole-brain structural connectivity in dyskinetic cerebral palsy and its association with motor and cognitive function. *Hum Brain Mapp.* 2017;38(9):4594-4612.
 15. Laporta-Hoyos O, Pannek K, Ballester-Plané J, et al. White matter integrity in dyskinetic cerebral palsy: relationship with intelligence quotient and executive function. *NeuroImage Clin.* 2017;15:789-800.
 16. Yoshida S, Faria AV, Oishi K, et al. Anatomical characterization of athetotic and spastic cerebral palsy using an atlas-based analysis. *J Magn Reson Imaging.* 2013;38(2):288-298.
 17. Purves D. *Neurociencia.* 5th ed. Medica Panamericana; 2016.
 18. Maillieux L, Franki I, Emsell L, et al. The relationship between neuroimaging and motor outcome in children with cerebral palsy: a systematic review-part B diffusion imaging and tractography. *Res Dev Disabil.* 2020;97:103569.
 19. Yoshida S, Hayakawa K, Oishi K, et al. Athetotic and spastic cerebral palsy: anatomic characterization based on diffusion-tensor imaging. *Radiology.* 2011;260(2):511-520.
 20. Harlaar L, Pouwels P, Geytenbeek J, Oostrom K, Barkhof F, Vermeulen R. Language comprehension in young people with severe cerebral palsy in relation to language tracts: a diffusion tensor imaging study. *Neuropediatrics.* 2013;44(5):286-290.
 21. Park BH, Park SH, Seo JH, Ko MH, Chung GH. Neuroradiological and neurophysiological characteristics of patients with dyskinetic cerebral palsy. *Ann Rehabil Med.* 2014;38(2):189-199.
 22. Bleyenheuft Y, Dricot L, Ebner-Karestinis D, et al. Motor skill training may restore impaired corticospinal tract fibers in children with cerebral palsy. *Neurorehabil Neural Repair.* 2020;34(6):533-546.
 23. Laporta-Hoyos O, Fiori S, Pannek K, et al. Brain lesion scores obtained using a simple semi-quantitative scale from MR imaging are associated with motor function, communication and cognition in dyskinetic cerebral palsy. *NeuroImage Clin.* 2018;19:892-900.
 24. Toronto AS. *Screening Test of Spanish Grammar.* Northwestern University Press; 1973.
 25. Palisano R, Rosenbaum P, Walter S, Russell D, Wood E, Galuppi B. Development and reliability of a system to classify gross motor function in children with cerebral palsy. *Dev Med Child Neurol.* 1997;39(4):214-223.
 26. Palisano RJ, Rosenbaum P, Bartlett D, Livingston MH. Content validity of the expanded and revised gross motor function classification system. *Dev Med Child Neurol.* 2008;50(10):744-750.
 27. Elvrum AKG, Andersen GL, Himmelmann K, et al. Bimanual fine motor function (BFMF) classification in children with cerebral palsy: aspects of construct and content validity. *Phys Occup Ther Pediatr.* 2014;36(1):1-16.
 28. Eliasson AC, Krumlinde-Sundholm L, Rösblad B, et al. The manual ability classification system (MACS) for children with cerebral palsy: scale development and evidence of validity and reliability. *Dev Med Child Neurol.* 2006;48(7):549-554.
 29. Pannek K, Guzzetta A, Colditz PB, Rose SE. Diffusion MRI of the neonate brain: acquisition, processing and analysis techniques. *Pediatr Radiol.* 2012;42(10):1169-1182.
 30. Pannek K, Boyd RN, Fiori S, Guzzetta A, Rose SE. Assessment of the structural brain network reveals altered connectivity in children with unilateral cerebral palsy due to periventricular white matter lesions. *NeuroImage Clin.* 2014;5:84-92.
 31. Tournier J-D, Smith R, Raffelt D, et al. MRtrix3: a fast, flexible and open software framework for medical image processing and visualisation. *NeuroImage.* 2019;202:116137.
 32. Avants BB, Epstein CL, Grossman M, Gee JC. Symmetric diffeomorphic image registration with cross-correlation: evaluating automated labeling of elderly and neurodegenerative brain. *Med Image Anal.* 2008;12(1):26-41.
 33. Makris N, Goldstein JM, Kennedy D, et al. Decreased volume of left and total anterior insular lobule in schizophrenia. *Schizophr Res.* 2006;83(2-3):155-171.
 34. Frazier JA, Chiu S, Breeze JL, et al. Structural brain magnetic resonance imaging of limbic and thalamic volumes in pediatric bipolar disorder. *Am J Psychiatry.* 2005;162(7):1256-1265.
 35. Desikan RS, Ségonne F, Fischl B, et al. An automated labeling system for subdividing the human cerebral cortex on MRI scans into gyral based regions of interest. *NeuroImage.* 2006;31(3):968-980.

36. Goldstein JM, Seidman LJ, Makris N, et al. Hypothalamic abnormalities in schizophrenia: sex effects and genetic vulnerability. *Biol Psychiatry*. 2007;61(8):935-945.
37. Eickhoff SB, Stephan KE, Mohlberg H, et al. A new SPM toolbox for combining probabilistic cytoarchitectonic maps and functional imaging data. *NeuroImage*. 2005;25(4):1325-1335.
38. Eickhoff SB, Heim S, Zilles K, Amunts K. Testing anatomically specified hypotheses in functional imaging using cytoarchitectonic maps. *NeuroImage*. 2006;32(2):570-582.
39. Eickhoff SB, Paus T, Caspers S, et al. Assignment of functional activations to probabilistic cytoarchitectonic areas revisited. *NeuroImage*. 2007;36(3):511-521.
40. Reid LB, Cespedes MI, Pannek K. How many streamlines are required for reliable probabilistic tractography? Solutions for microstructural measurements and neurosurgical planning. *NeuroImage*. 2020;211:116646.
41. Leisman G, Braun-Benjamin O, Melillo R. Cognitive-motor interactions of the basal ganglia in development. *Front Syst Neurosci*. 2014;8:8.
42. Cohen J. *Statistical Power Analysis for the Behavioral Sciences*. Rev ed. Lawrence Erlbaum Associates; 1988.
43. Bekteshi S, Vanmechelen I, Konings M, Ortibus E, Feys H, Monbaliu E. Clinical presentation of spasticity and passive range of motion deviations in Dyskinetic cerebral palsy in relation to dystonia, Choreoathetosis, and functional classification systems. *Dev Neurorehabil*. 2021;24(3):205-213.
44. Reid SM, Meehan EM, Reddihough DS, Harvey AR. Dyskinetic vs spastic cerebral palsy: a cross-sectional study comparing functional profiles, comorbidities, and brain imaging patterns. *J Child Neurol*. 2018;33(9):593-600.
45. Harrington DL, Jahanshahi M. Reconfiguration of striatal connectivity for timing and action. *Curr Opin Behav Sci*. 2016;8:78-84.
46. Lee J, Muzio MR. *Neuroanatomy, extrapyramidal system*. StatPearls. StatPearls Publishing; 2022.
47. Shabbott B. Learning fast accurate movements requires intact frontostriatal circuits. *Front Hum Neurosci*. 2013; 13: 752.
48. Visser JE, Bloem BR. Role of the basal ganglia in balance control. *Neural Plast*. 2005;12(2-3):161-174.
49. Monbaliu E, De La Peña MG, Ortibus E, et al. Functional outcomes in children and young people with dyskinetic cerebral palsy. *Dev Med Child Neurol*. 2017; 59(6): 634-640.
50. Carnahan KD, Arner M, Häggglund G. Association between gross motor function (GMFCS) and manual ability (MACS) in children with cerebral palsy. A population-based study of 359 children. *BMC Musculoskelet Disord*. 2007;8(1):50.
51. Jiang H, Liu H, He H, et al. Specific white matter lesions related to motor dysfunction in spastic cerebral palsy: a meta-analysis of diffusion tensor imaging studies. *J Child Neurol*. 2020;35(2):146-154.
52. Gupta D, Barachant A, Gordon AM, et al. Effect of sensory and motor connectivity on hand function in pediatric hemiplegia. *Ann Neurol*. 2017;82(5):766-780.
53. Jeurissen B, Leemans A, Tournier JD, Jones DK, Sijbers J. Investigating the prevalence of complex fiber configurations in white matter tissue with diffusion magnetic resonance imaging. *Hum Brain Mapp*. 2013;34(11):2747-2766.
54. Papadelis C, Kaye H, Shore B, Snyder B, Grant PE, Rotenberg A. Maturation of corticospinal tracts in children with hemiplegic cerebral palsy assessed by diffusion tensor imaging and transcranial magnetic stimulation. *Front Hum Neurosci*. 2019;13:254.
55. Papadelis C, Ahtam B, Nazarova M, et al. Cortical somatosensory reorganization in children with spastic cerebral palsy: a multimodal neuroimaging study. *Front Hum Neurosci*. 2014;8:725.
56. Papadelis C, Butler EE, Rubenstein M, et al. Reorganization of the somatosensory cortex in hemiplegic cerebral palsy associated with impaired sensory tracts. *NeuroImage Clin*. 2018;17:198-212.
57. Jaatela J, Aydogan DB, Nurmi T, Vallinoja J, Mäenpää H, Piitulainen H. Limb-specific thalamocortical tracts are impaired differently in hemiplegic and diplegic subtypes of cerebral palsy. *Cereb Cortex*. 2023;33(19):10245-10257.
58. Reid LB, Cunnington R, Boyd RN, Rose SE. Surface-based fMRI-driven diffusion Tractography in the presence of significant brain pathology: a study linking structure and function in cerebral palsy. *PLoS One*. 2016;11(8):e0159540.
59. Reid LB, Pagnozzi AM, Fiori S, Boyd RN, Dowson N, Rose SE. Measuring neuroplasticity associated with cerebral palsy rehabilitation: an MRI based power analysis. *Int J Dev Neurosci*. 2017;58:17-25.
60. Figley CR, Uddin MN, Wong K, Kornelsen J, Puig J, Figley TD. Potential pitfalls of using fractional anisotropy, axial diffusivity, and radial diffusivity as biomarkers of cerebral white matter microstructure. *Front Neurosci*. 2022;15:15.
61. Winkiewski PJ, Sabisz A, Naumczyk P, Jodzio K, Szurowska E, Szarmach A. Understanding the physiopathology behind axial and radial diffusivity changes-what do we know? *Front Neurol*. 2018;9:92.
62. Wheeler-Kingshott CAM. Technology-driven progress. *Funct Neurol*. 2012;27(3):129.
63. Monbaliu E, Ortibus E, De Cat J, et al. The dyskinesia impairment scale: a new instrument to measure dystonia and choreoathetosis in dyskinetic cerebral palsy. *Dev Med Child Neurol*. 2012;54(3):278-283.

Supporting Information

Additional supporting information may be found online in the Supporting Information section at the end of the article.

Data S1.